Journal of Thermal Analysis and Calorimetry, Vol 88 (2007) 3, 717–722

KINETICS OF THERMAL OXIDATION OF TITANIUM CARBIDE AND ITS CARBON NANO-COMPOSITES IN DRY AIR ATMOSPHERE

A. Biedunkiewicz[1], N. Gordon[2], J. Straszko[3] and S.Tamir[2]*

[1]Institute of Materials Science and Engineering, Szczecin University of Technology
[2]Israel Institute of Metals, Technion, Haifa
[3]Institute of Chemistry and Environmental Protection, Szczecin University of Technology

Results of research work on oxidation of TiC/C nano-composites in air and under non-isothermal conditions are presented.

The oxidation of nano-crystalline titanium carbide as well as its carbon composites were studied using TG-DSC method in dry air atmosphere. The investigated samples were as follows: commercial TiC nano-powders from Alfa Aesar (80 nm) and carbon composites including nano-crystalline TiC (30 nm and 50, 10, 3 mass% of carbon in matrix). The measurements were executed in the Setaram thermoanalyser TG-DSC 92-15 in non-isothermal conditions, with mass samples of 30±0.2 mg and constant heating rate in the range 2–10 K min^{-1}.

During the oxidation experiments the heat flux (HF), thermogravimetric and derivative thermogravimetric curves were recorded. The $g(\alpha)$ functions (kinetic models), kinetic parameters of the Arrhenius equation A and E, dependencies of conversion degree on time were determined. Comparison of oxidation rates of different TiC nanomaterials was made.

Keywords: *carbon nano-composites, oxidation kinetics, thermal analysis, titanium carbide*

Introduction

Nano-materials, due to their enhanced physical properties, are attractive for various applications. The TiC particles have high hardness and strength along with resistance to heat, corrosion and wear. Additionally, they exhibit good electrical and thermal conductivity. However, widespread use of TiC has been limited due to their inherent brittleness and catastrophic failure mode at low temperature. One possibility to improve TiC mechanical properties might be the reduction of crystallite sizes down to the nano-sized range. Nano-structured ceramics show several important mechanical modifications like superplasticity, increased strength, diffusivity, higher thermal expansion coefficient, lower thermal conductivity, reduced density, improved toughness, etc. [1, 2]. Sintering of nanoparticles indicated depressed sintering onset temperatures (0.2–0.3 T_m) as compared to conventional powders (0.5–0.8 T_m) [3].

Many researches have been conducted on oxidation process of several transition metal carbides, mainly single crystals and powders. A review of the state of knowledge on the TiC oxidation has been described in this article [4].

Quantitative description of a kinetic process is underlied by its mechanism. Shimada and Kozeki proposed the following mechanism for metal carbides oxidation which is in general accepted today. The oxidation occurs through the following four stages.

At first stage the dissolved oxygen reacts with carbide forming the first oxycarbide layer according to the equation:

$$MEC+3/2xO_2 \rightarrow MEC_{1-x}O_x + xCO_2 \quad (1)$$

As a result layer 1 appears on the carbide surface. At second stage the elemental carbon is evolved according to Eq. (2) and forms the amorphous layer of metal dioxide MEO_2:

$$MEC_{1-x}O_x + (1-x/2)O_2 \rightarrow MEO_2 + (1-x)C \quad (2)$$

In stage III amorphous MeO_2, produced in reaction (2), crystallizes, and starts forming layer 2. This layer is porous due to the higher molar volume of products than TiC. As a result cracks occur in this layer which support transport of oxygen from gaseous phase to reaction zone.

In stage IV, which takes place after forming the both layers, oxidation of substrates occurs.. This reaction proceeds under porous layer of oxides. As a result amorphous, non-porous layer of oxides adjacent to MeC surface is regenerated. This phenomenon lowers the rate of the process and can even bring it to stop. In discussed stage a combustion of carbon educed in the second stage also takes place.

$$C+O_2 \rightarrow CO_2 \quad (3)$$

* Author for correspondence: anna.biedunkiewicz@ps.pl

1388–6150/$20.00

Akadémiai Kiadó, Budapest, Hungary
Springer, Dordrecht, The Netherlands

According to the kinetic research conducted by Shimada and other authors, under isothermal conditions usually two steps are observed. The first stage consists of forming layer I and proceeds according to the parabolic kinetics equation. The second stage starts after formation of both layers and during this step oxygen diffuses to layer I in which the reaction proceeds. This stage is described in literature by linear equation. It should be underlined that given kinetic dependencies were obtained after assuming by authors a certain way of expressing conversion degree.

It also should be noticed that, depending on temperature and oxygen partial pressure in gaseous mixtures, a few processes may take part in forming the layer I. In low temperature and under low p_{O_2} there can be one process described by Eq. (1) or two processes up to the formulas (1) and (2). In higher temperature and p_{O_2} the first stage may consists of three processes (reactions (1), (2) and crystallisation of amorphous MeO_2 formed in reaction (2)). This hampers quantitative description of the process.

Experimental

Materials and methods

The oxidation of nano-crystalline titanium carbide, commercial powders (Alfa Aesar 80 nm) in dry air was studied as well as of carbon composites including nano-crystalline TiC (30 nm and 50, 10, 3 mass% of carbon in matrix) obtained by nonhydrolytic sol-gel method [6]. The following techniques were applied for the samples characterization: scanning electron microscopy (JEOL JSM 6100), transmission electron microscopy (JEOL JEM 1200EX) and X-ray diffraction (PHILIPS PW3710). The following parameters of XRD measurements were applied: Copper X-ray tube (λ=1.5406 Å), high voltage 40 kV and current 0.040 A. Average crystallite size was measured according to the Sherrer formula:

$$t=\frac{0.9\lambda}{B\cos\theta_B}$$

where t – average grain size, B – peak width at half intensity, λ – X-ray wavelength, θ_B – peak angle (Radians).

The HF, DTG and TG curves were recorded. The measurements were executed in the Setaram theromoanalyser TG-DSC 92-15 in non-isothermal conditions, with constant heating rates in the range 2–10 K min^{-1}. Samples of 30±0.2 mg were used. The conversion degrees dependence on temperature $\alpha(T)$ basing on the experimental data was determined.

Additionally the TiC particles' surface was modified by oxidation in a furnace with continues air flow. TiC nano-particles from Alfa Aesar were oxidized at 350°C for 30 min, in order to partially oxidize the TiC to TiO_2. Carbon/TiC composite particles were oxidized at 450 and 550°C for 30 min.

In quantitative description every stage has been treated as a separate conversion. Reaction rate generally depends on conversion degree and temperature

$$r=\frac{d\alpha}{dt}=f(T,\alpha) \tag{4}$$

In kinetic data analysis it is assumed that the rate of reaction r=dα/dt can be shown as a combination of two functions $k(T)$ and $f(\alpha)$, where the first one is the Arrhenius equation and the function $f(\alpha)$ means the reaction kinetic model

$$r=k(T)f(\alpha) \tag{5}$$

Dependence of reaction rate constant on temperature is expressed by the Arrhenius equation

$$k(T)=A\exp\left\{-\frac{E}{RT}\right\} \tag{6}$$

Non-isothermal measurements are conducted under linear increase of temperature and constant heating rate

$$T=T_0+\beta t \tag{7}$$

After substitution of Eqs (7) and (6) into Eq. (5) one obtains equation where the independent variable is temperature:

$$\frac{d\alpha}{dT}=\frac{A}{\beta}\exp\left\{-\frac{E}{RT}\right\}f(\alpha) \tag{8}$$

After rearrangement of Eq. (8) and integration we get

$$g(\alpha)=\int\frac{d\alpha}{f(\alpha)}=\frac{A}{\beta}\int\exp\left\{-\frac{E}{RT}\right\}dT \tag{9}$$

The integral on the right side of Eq. (9) does not have any analytical solution. Various approximations are being applied. Good results are given by the Coats and Redfern equation

$$\ln\left(\frac{g(\alpha)}{T^2}\right)=\ln\left\{\frac{AR}{\beta E}\left(1-\frac{2RT_m}{E}\right)\right\}-\frac{E}{RT} \tag{10}$$

where

A	pre-exponential Arrhenius factor, min^{-1}
E	apparent activation energy, kJ mol^{-1}
ΔG^*	Gibbs free energy of activated complexes, kJ mol^{-1}
ΔH^*	enthalpy of activated complexes, kJ mol^{-1}
ΔS^*	entropy of activated complexes, kJ mol^{-1} K^{-1}
h	Planck constant
$k(T)$	rate constant, min^{-1}
k_B	Boltzmann constant

R gas constant, kJ mol^{-1} K^{-1}
r reaction rate, min^{-1}
t time, min
T temperature, K
T_0 initial temperature for a series of measurements, K
T_m maximum conversion rate temperature for a stage, K
α conversion degree
β sample heating rate, K min^{-1}
$f(\alpha)$ conversion function dependent on mechanism of reaction,
$g(\alpha)$ integral form of the conversion function.

In the study of measurements for every stage a figure of function $g(\alpha)$ (the kinetic model of process) bestly refering to the experimental data was chosen, then the parameters A, E were marked. The identification of the kinetic models was executed with the use of statistical methods. Authors emphasize that the appointed figures of function $g(\alpha)$ were treated as dependence bestly corresponding to the experimental data, and A and E as function parameters. With regard to the internal variation of real processes and the mismeasurements the variables occurring in the Eq. (10) were treated as random variables, and the reaction of TiC oxidation as a stochastic process. The methodology of kinetic models identification was published in these works [4, 6].

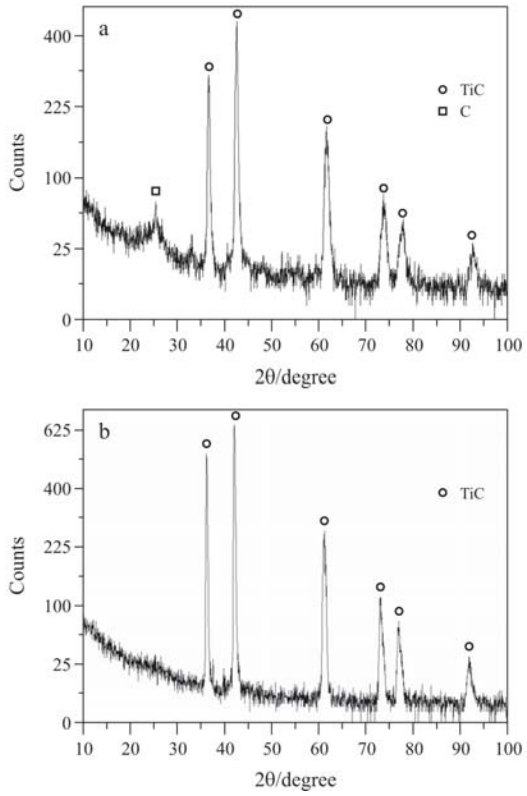

Fig. 1 XRD pattern of the TiC/C nano-composite; 30 nm of TiC size with a – 50 mass% of carbon matrix and b – 3 mass% of carbon cages

Results and discussion

The X-ray powder diagram and scanning images of TiC/C composite powder prepared by the sol-gel method is presented in Figs 1 and 2. It is visible the powder contains two crystalline phases: graphite and titanium carbide.

The TEM observations and XRD measurements of TiC particles showed that they formed with a grain size below 30 nm – Fig. 3.

Figures 4 and 5 present TG and HF graphs for nano-crystalline titanium carbide, sizes of 80 nm, and Figs 6 and 7 for nano-composite TiC/C.

For all series of measurements of studied materials the calculations were done [4, 6]. Results were summarized in Table 1.

The knowledge of kinetic models enables to evaluate the kinetics of oxidation process of *n*-TiC as well as *n*-TiC/C in the air in isothermal conditions. Integrating Eq. (5) we obtain:

$$g(\alpha)=\int\frac{d\alpha}{f(\alpha)}=k(T)t \qquad (11)$$

Equation (11) is the basis for analysis of process. For selected materials calculations of the dependence of conversion degree *vs.* temperature and time were carried out. The variation range of conversion degree was fixed on $0.01<\alpha<0.99$. For the given values the $f(\alpha)$ and $g(\alpha)$

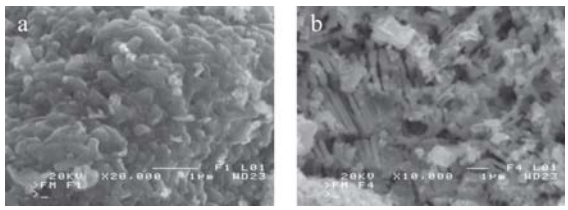

Fig. 2 SEM images of the TiC/C nano-composite; 30 nm of TiC size with a – 50 mass% of carbon matrix and b –3 mass% of carbon cages

Fig. 3 TEM image of the *n*-TiC in carbon cages (30 nm, 3 mass% of C matrix)

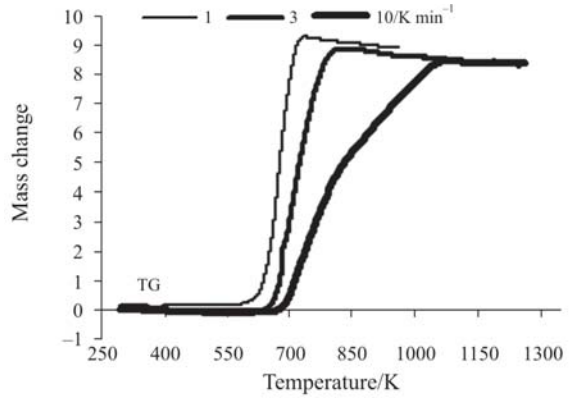

Fig. 4 Comparison of TG curves. Oxidation of TiC (80 nm) in air

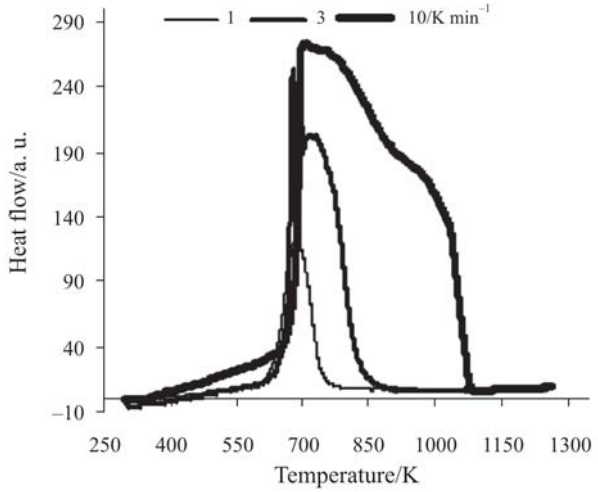

Fig. 5 Comparison of HF curves. Oxidation of TiC (80 nm) in air

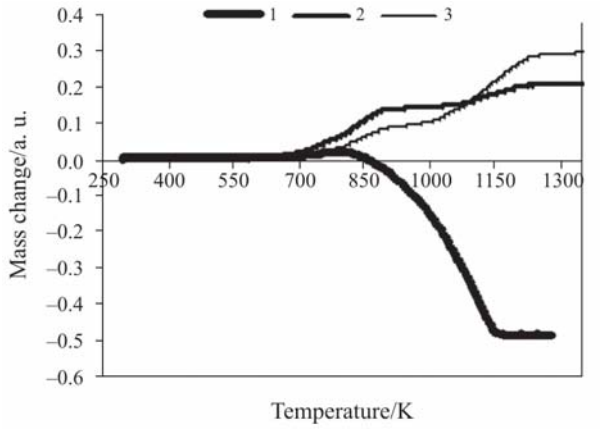

Fig. 6 Comparison of TG curves. Oxidation of TiC/C nano-composites (30 nm) in air. 50, 10, 3 mass% of the carbon contents in composites signet 1, 2, 3, respectively

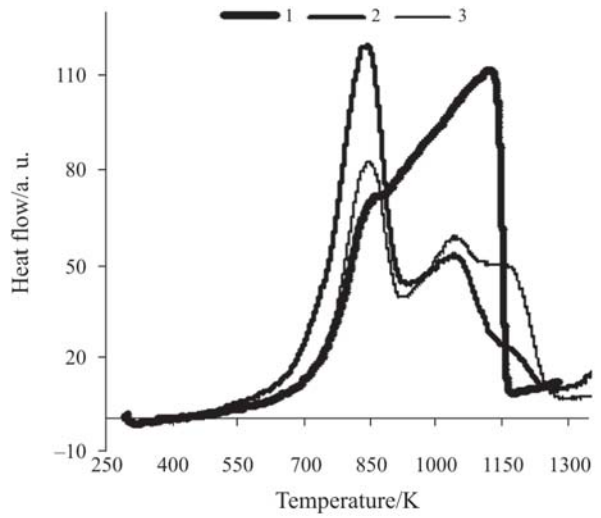

Fig. 7 Comparison of HF curves. Oxidation of TiC/C nano-composites (30 nm) in air. 50, 10, 3 mass% of the carbon contents in composites signet 1, 2, 3, respectively

were calculated. Then, for certain temperatures, applying the value of parameters A and E, the heating rate values $k(T)$ were calculated. Basing on the value of $g(\alpha)$ and the $k(T)$, the time needed for establishing the conversion degree was calculated. Calculations were carried out for all studied materials and at following temperatures: 823; 1000 K.

To facilitate the comparison of dependence of conversion degree on time and temperature, summary diagrams were done. In Figs 8 and 9 results were introduced, correspondently, for temperatures 823 and 1000 K. Commercial TiC is very reactive, therefore to show the dependence, the scale of time and temperature was reduced.

It can be observed that the reactivity of studied materials varies, and the time to obtain a comparable conversion degree varies too. A position shift occurs in the curves. It is related to different energy of activation of the examined processes.

Table 1 Kinetics parameters and models for the materials

Materials	Model	$f(\alpha)$	$g(\alpha)$	A/min^{-1}	E/kJ mol^{-1}
TiC (80 nm)	F1	$(1-\alpha)$	$[-\ln(1-\alpha)]$	8.29E07	126.75
TiC/C (30 nm, 50 mass% of C)	F1	$(1-\alpha)$	$[-\ln(1-\alpha)]$	3.15E04	117.27
TiC/C (30 nm, 10 mass% of C)	F2	$(1-\alpha)^2$	$(1-\alpha)^{-1}-1$	6.416E03	81.75
TiC/C(30 nm, 3 mass% of C)	F1	$(1-\alpha)$	$[-\ln(1-\alpha)]$	2.86E01	68.53

In temperature of 1000 K as compared to 823 K the time necessary to obtain a total conversion is much shorter. At all stages a high reactivity of commercial TiC is visible. In the other cases its reactivity depends on the carbon matrix of the nano-crystalline.

TiC nano-particles from Alfa Aesar and composite carbon/TiC were oxidized in order to partially oxidize the TiC to TiO_2. X-ray analysis detected two phases of TiO_2–rutile (tetragonal) and anatase (monoclinic) – Fig. 11. TiC (Alfa Aesar) grain size decreased from about 75 to about 50 nm due to the oxidation process according to X-ray grain size analysis. Results of the experiments were compared to the determined dependencies of conversion degree on time. For the nano-particles oxidized at 350°C for 30 min the conversion degree equals α=0.08. It is consistent with the analytically determined value from $\alpha=f$(time) – Fig. 10.

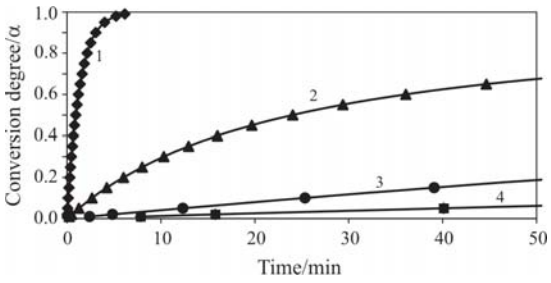

Fig. 8 Dependence of conversion degree on time – $\alpha(t)$. T=823 K. 1 – TiC commercial (80 nm); 2 – TiC/C (30 nm, 10 mass% of C); 3 – TiC/C (20 nm, 50 mass% of C); 4 – TiC/C (30 nm, 3 mass% of C)

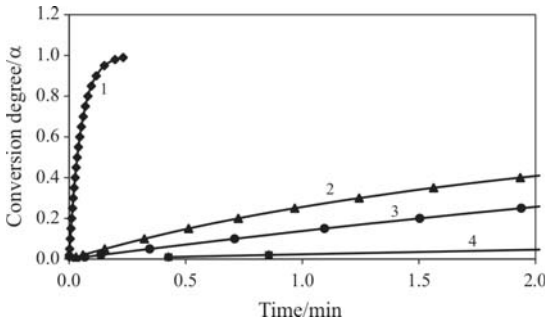

Fig. 9 Dependence of conversion degree on time – $\alpha(t)$. T=1000 K. 1 – TiC commercial (80 nm); 2 – TiC/C (30 nm, 10 mass% of C); 3 – TiC/C (20 nm, 50 mass% of C); 4 – TiC/C (30 nm, 3 mass% of C)

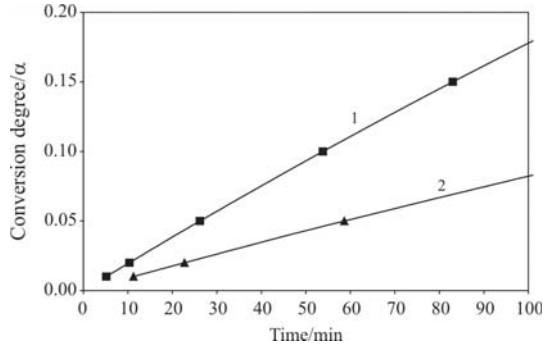

Fig. 10 Dependence of conversion degree $\alpha(t)$ – on time. T=623 K. 1 – TiC commercial (80 nm); 2 – TiC/C (30 nm, 10 mass% of C)

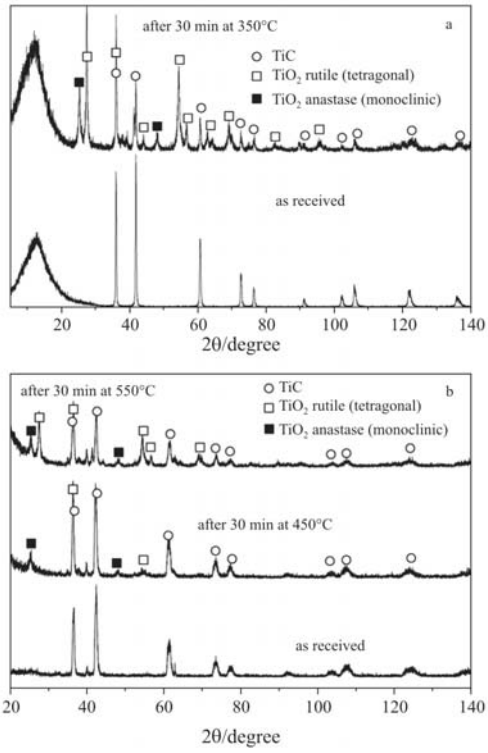

Fig. 11 XRD analysis of a – nano-TiC Alfa Aesar (80 nm) and b – TiC/C nano-composite before and after oxidation process

Conclusions

The present study shows that the oxidation rate of nanocrystalline TiC in carbon matrices decreases along with the carbon content in the matrix. Comparison of conversion degrees of isothermal oxidation processes of commercial nanocrystalline TiC with TiC/C nanocomposites leads to the conclusion that carbon matrix protects TiC crystallites from air oxidation.

It was stated that the appointed dependence of α functions on time are in good correspondence with experimental results. The experimental verification in the example of the commercial TiC nanocrystallites oxidation at 623 K was illustrated in this paper.

Acknowledgements

This paper and the work it concerns were generated in the context of the MULTIPROTECT project, funded by the European Community as contract N^0 NMP3-CT-2005-011783 under the 6^{th} Framework Programme for Research and Technological Development.

References

1 F. Wakai, N. Kondo, H. Ogawa, T. Nagano and S. Tsurekawa, Mater. Charact., 37 (1996) 331.
2 M. Gell, Mater. Sci. Eng., A204 (1995) 246.
3 J. R. Groza, Nanostruct. Mater., 12 (1999) 987.
4 A. Biedunkiewicz, A. Strzelczak and J. Chrościechowska, Polish J. Chem. Technol., 7 (2005) 1.
5 S. Shimada and M. Kozeki, J. Mater. Sci., 27 (1992) 1869.
6 A. Biedunkiewicz, Mater. Sci., 21 (2003) 445.

DOI: 10.1007/s10973-006-8222-x